CMB Lensing Reconstruction on the Full Sky

Takemi Okamoto
Department of Physics and the Center for Cosmological Physics, University of Chicago, Chicago, IL 60637[*]

Wayne Hu
Center for Cosmological Physics and the Department of Astronomy and Astrophysics and the Enrico Fermi Institute, University of Chicago, Chicago, IL 60637[†]

(Dated: January 3, 2003)

Gravitational lensing of the microwave background by the intervening dark matter mainly arises from large-angle fluctuations in the projected gravitational potential and hence offers a unique opportunity to study the physics of the dark sector at large scales. Studies with surveys that cover greater than a percent of the sky will require techniques that incorporate the curvature of the sky. We lay the groundwork for these studies by deriving the full sky minimum variance quadratic estimators of the lensing potential from the CMB temperature and polarization fields. We also present a general technique for constructing these estimators, with harmonic space convolutions replaced by real space products, that is appropriate for both the full sky limit and the flat sky approximation. This also extends previous treatments to include estimators involving the temperature-polarization cross-correlation and should be useful for next generation experiments in which most of the additional information from polarization comes from this channel due to sensitivity limitations.

I. INTRODUCTION

Weak gravitational lensing of the microwave background anisotropies offers a unique opportunity to study the dark matter and energy distribution at intermediate redshifts and large scales. In addition to producing modifications in the CMB temperature and polarization power spectra [1, 2], lensing of the CMB fields produces higher-order correlations between the multipole moments [3, 4]. Quadratic combinations of the CMB fields can be used to form estimators of the projected gravitational potential, and therefore of the projected mass [5, 6]. The minimum variance quadratic estimator can in principle map the projected mass on large angular scales out to multipole moments of $L \sim 10^2$ [7, 8] and contains nearly all of the information in the higher moments of the lensed temperature field [9]. Substantially more information lies in the lensed polarization fields allowing high signal-to-noise lensing reconstruction and extending the angular resolution out to $L \sim 10^3$ [10].

Lensing reconstruction techniques involving the polarization fields have previously only been developed for small surveys where the sky can be taken to be approximately flat. Since lensing is intrinsically most sensitive to the projected potential at $L < 10^2$ or several degrees on the sky, a treatment incorporating the curvature of the sky is desirable. In fact it is necessary for its application in removing the lensing contaminant to gravitational wave polarization [10, 11, 12] across large regions of the sky.

We present a concise treatment of the effect of gravitational lensing on CMB temperature and polarization harmonics in Sect. II. We construct the full sky quadratic estimators of the lensing potential and compare their noise properties to that for the flat sky expressions in Sect. III. We provide an efficient algorithm for the construction of all estimators in Sect. IV. We derive the flat sky limits of the estimators and draw the connection to results in [10] in Sect. V. We summarize some useful properties of spin-weighted functions in Appendix A.

II. CMB LENSING IN MULTIPOLE SPACE

In this section, we give a pedagogical but concise derivation of the lensing effect on the CMB temperature and polarization fields on the sphere [13, 14]. We emphasize the connections between the formalism using spin-weighted spherical harmonics [15] and a tensorial approach [16] which will be useful for the lensing reconstruction in the following sections.

---

[*]Electronic address: tokamoto@oddjob.uchicago.edu
[†]Electronic address: whu@background.uchicago.edu

The temperature perturbation is characterized by a scalar function $\Theta(\hat{\boldsymbol{n}}) \equiv \Delta T(\hat{\boldsymbol{n}})/T$, whose harmonic transform is given by

$$\Theta(\hat{\boldsymbol{n}}) \equiv \sum_{lm} \Theta_l^m Y_l^m(\hat{\boldsymbol{n}}). \tag{1}$$

The polarization anisotropy of the microwave background is characterized by a traceless, symmetric rank 2 tensor, which can be represented as (e.g. [16])

$$\boldsymbol{\mathcal{P}}_{ij} = {}_{+2}A(\hat{\boldsymbol{n}})\bar{\boldsymbol{m}}_i\bar{\boldsymbol{m}}_j + {}_{-2}A(\hat{\boldsymbol{n}})\boldsymbol{m}_i\boldsymbol{m}_j, \tag{2}$$

where we have defined the complex Stokes parameters ${}_{\pm2}A$ according to

$$_{\pm2}A(\hat{\boldsymbol{n}}) \;=\; Q(\hat{\boldsymbol{n}}) \pm iU(\hat{\boldsymbol{n}}). \tag{3}$$

The spin projection vectors are given with respect to the measurement basis $(\hat{\boldsymbol{e}}_1, \hat{\boldsymbol{e}}_2)$ by

$$\boldsymbol{m} \;=\; \frac{1}{\sqrt{2}}\left[\hat{\boldsymbol{e}}_1 + i\hat{\boldsymbol{e}}_2\right], \tag{4}$$

$$\bar{\boldsymbol{m}} \;=\; \frac{1}{\sqrt{2}}\left[\hat{\boldsymbol{e}}_1 - i\hat{\boldsymbol{e}}_2\right], \tag{5}$$

and form an eigenbasis under local rotations of basis vectors (see Appendix A). In spherical polar coordinates, $\hat{\boldsymbol{e}}_1 = \hat{\boldsymbol{e}}_\theta$ and $\hat{\boldsymbol{e}}_2 = \hat{\boldsymbol{e}}_\phi$. Under a local, right-handed rotation of the basis $(\hat{\boldsymbol{e}}_1, \hat{\boldsymbol{e}}_2)$ by an angle ψ, the complex Stokes parameters ${}_{\pm2}A(\hat{\boldsymbol{n}})$ acquire a phase $e^{\mp 2i\psi}$. They act as spin-2 functions, with a corresponding harmonic transform in terms of spin-weighted spherical harmonics [17] given by [15]

$$_{\pm2}A(\hat{\boldsymbol{n}}) \equiv \sum_{lm} {}_{\pm2}A_l^m \, {}_{\pm2}Y_l^m(\hat{\boldsymbol{n}}). \tag{6}$$

A lens with a projected potential $\phi(\hat{\boldsymbol{n}})$ maps the temperature and polarization anisotropies according to [2, 3, 18]

$$\begin{aligned}\Theta(\hat{\boldsymbol{n}}) &= \tilde{\Theta}(\hat{\boldsymbol{n}} + \nabla\phi(\hat{\boldsymbol{n}})) \\ &= \tilde{\Theta}(\hat{\boldsymbol{n}}) + \nabla_i\phi(\hat{\boldsymbol{n}})\nabla^i\tilde{\Theta}(\hat{\boldsymbol{n}}) + \mathcal{O}(\phi^2), \end{aligned} \tag{7}$$

$$\begin{aligned}\boldsymbol{\mathcal{P}}_{ij}(\hat{\boldsymbol{n}}) &= \tilde{\boldsymbol{\mathcal{P}}}_{ij}(\hat{\boldsymbol{n}} + \nabla\phi(\hat{\boldsymbol{n}})) \\ &= \tilde{\boldsymbol{\mathcal{P}}}_{ij}(\hat{\boldsymbol{n}}) + \nabla_k\phi(\hat{\boldsymbol{n}})\nabla^k\tilde{\boldsymbol{\mathcal{P}}}_{ij}(\hat{\boldsymbol{n}}) + \mathcal{O}(\phi^2), \end{aligned} \tag{8}$$

where tildes denote the unlensed fields. In the case of a weak gravitational field under consideration, lensing potential ϕ is obtained by a line-of-sight projection of the gravitational potential,

$$\phi(\hat{\boldsymbol{n}}) = -2\int d\eta \frac{\chi(\eta - \eta_s)}{\chi(\eta_s)\chi(\eta)}\Psi(\chi\hat{\boldsymbol{n}}, \eta), \tag{9}$$

where η is the conformal time, η_s is the epoch of last scattering and χ is the angular diameter distance in comoving coordinates.

Taking the harmonic transform of Eqn. (7), one readily shows that the the change to the temperature moments $\delta\Theta_l^m \equiv \Theta_l^m - \tilde{\Theta}_l^m$ are given by [19]

$$\delta\Theta_l^m \;\approx\; \sum_{LM}\sum_{l'm'} \phi_L^M \tilde{\Theta}_{l'}^{m'} I_{lLl'}^{mMm'}, \tag{10}$$

with $I_{lLl'}^{mMm'}$ denoting the integral

$$I_{lLl'}^{mMm'} \;=\; \int d\hat{\boldsymbol{n}} Y_l^{m*}\nabla_i Y_L^M \nabla^i Y_{l'}^{m'}. \tag{11}$$

The integral can be performed analytically to yield

$$I_{lLl'}^{mMm'} = (-1)^m \begin{pmatrix} l & L & l' \\ -m & M & m' \end{pmatrix} {}_0F_{lLl'}, \tag{12}$$

with the general definition

$$ {}_{\pm s}F_{lLl'} = [L(L+1) + l'(l'+1) - l(l+1)] \sqrt{\frac{(2L+1)(2l+1)(2l'+1)}{16\pi}} \begin{pmatrix} l & L & l' \\ \pm s & 0 & \mp s \end{pmatrix}. \tag{13} $$

The multipole expansion for the polarization fields proceeds by noting that ${}_{\pm 2}A(\hat{\boldsymbol{n}})$ are the spin ± 2 components of the polarization tensor $\boldsymbol{\mathcal{P}}_{ij}$. Since the contraction with the spin projection vectors $\boldsymbol{m}^i\boldsymbol{m}^j$ projects out the spin 2 piece of a symmetric tensor, the change in the complex Stokes parameters is given by

$$ \begin{aligned} \delta\left[{}_{+2}A(\hat{\boldsymbol{n}})\right] &= \boldsymbol{m}^i\boldsymbol{m}^j\delta\boldsymbol{\mathcal{P}}_{ij} \\ &\approx \boldsymbol{m}^i\boldsymbol{m}^j\left[\nabla_k\tilde{\boldsymbol{\mathcal{P}}}_{ij}(\hat{\boldsymbol{n}})\right]\left[\nabla^k\phi(\hat{\boldsymbol{n}})\right]. \end{aligned} \tag{14} $$

The expression for the contribution to ${}_{-2}A(\hat{\boldsymbol{n}})$ is obtained by replacing $\boldsymbol{m}^i$ by $\bar{\boldsymbol{m}}^i$ in the above. We denote the product $\boldsymbol{m}^i\boldsymbol{m}^j\nabla_k\tilde{\boldsymbol{\mathcal{P}}}_{ij}$ using a spin-gradient derivative D_i (see Eq. A12), and write the lensing contribution as

$$ \delta\left[{}_{\pm 2}A(\hat{\boldsymbol{n}})\right] \approx D^i\phi(\hat{\boldsymbol{n}})D_i[{}_{\pm 2}\tilde{A}(\hat{\boldsymbol{n}})]. \tag{15} $$

This relationship was given in [13] with the shorthand convention $D_i \to \nabla_i$ corresponding to the action of covariant derivatives on the spin components of symmetric trace free tensors given in Eqn. (A11) [14, 17]. Expanding ϕ and ${}_{\pm 2}A$ in spin-weighted spherical harmonics and evaluating the inner product of their gradients using Eqn. (A18), we obtain the lensing corrections

$$ \delta[{}_{\pm 2}A_l^m] \approx \sum_{LM}\sum_{l'm'} \phi_L^M \, {}_{\pm 2}\tilde{A}_l^m \, {}_{\pm 2}I_{lLl'}^{mMm'}, \tag{16} $$

where we define

$$ {}_{\pm 2}I_{lLl'}^{mMm'} = (-1)^m \begin{pmatrix} l & L & l' \\ -m & M & m' \end{pmatrix} {}_{\pm 2}F_{lLl'}. \tag{17} $$

We will be interested in the lensing expressions for the rotationally invariant combinations

$$ E_l^m = \frac{1}{2}\left[{}_{+2}A_l^m + {}_{-2}A_l^m\right], \tag{18} $$

$$ B_l^m = \frac{1}{2i}\left[{}_{+2}A_l^m - {}_{-2}A_l^m\right], \tag{19} $$

which are the curl-free ("E-mode") and gradient-free ("B-mode") components of the polarization field. From the expressions (10) and (16), we find the general expression for a lensed multipole moment to be

$$ \delta X_l^m \approx \sum_{LM}\sum_{l'm'} \phi_L^M (-1)^m \begin{pmatrix} l & l' & L \\ m & -m' & -M \end{pmatrix} {}_{s_X}F_{lLl'}\left[\epsilon_{ll'L}X_{l'}^{m'} + \beta_{ll'L}\bar{X}_{l'}^{m'}\right], \tag{20} $$

where X_l^m may be multipole moments of Θ, E, or B, and

$$ \begin{aligned} \epsilon_{ll'L} &= \frac{1+(-1)^{L+l+l'}}{2}, \\ \beta_{ll'lL} &= \frac{1-(-1)^{L+l+l'}}{2i} \end{aligned} \tag{21} $$

ensure that the associated terms are nonzero only when $L + l + l'$ is even or odd, respectively. $\bar{X}$ denotes the parity complement of X, i.e. $\bar{\Theta} = 0$, $\bar{E} = -B$, $\bar{B} = E$.

III. QUADRATIC ESTIMATORS

Lensing of the CMB fields mixes different multipoles through the convolution (20), and therefore correlates modes across a band determined by the power in the deflection angles [13]. The unlensed CMB fields $\tilde{X}_l^m$ are assumed to be Gaussian and statistically isotropic, so that the statistical properties are characterized by diagonal covariances or power spectra

$$\langle \tilde{X}_l^{m*} \tilde{X}'^{m'}_{l'} \rangle = \delta_{ll'} \delta_{mm'} \tilde{C}_l^{XX'} . \tag{22}$$

The assumption of parity invariance implies that $\tilde{C}_l^{\Theta B} = \tilde{C}_l^{EB} = 0$. The lensing potential is also assumed to be statistically isotropic so that

$$l(l+1) \langle \phi_l^{m*} \phi_{l'}^{m'} \rangle = \delta_{ll'} \delta_{mm'} C_l^{dd} . \tag{23}$$

where we have multiplied through by $l(l+1)$ to reflect the weighting of deflection angles.

It follows then that the lensed fields on the sky X_l^m are also statistically isotropic with power spectra

$$\langle X_l^{m*} X'^{m'}_{l'} \rangle = \delta_{ll'} \delta_{mm'} C_l^{XX'} . \tag{24}$$

Since X_l^m denotes the measured fields, the power spectra contain all sources to the variance, including detector noise. Detector noise will be taken to be homogeneous, with power spectra given by [20]

$$\begin{aligned} C_l^{\Theta\Theta}\big|_{\rm noise} &= \left(\frac{\Delta_\Theta}{T_{\rm CMB}} \right)^2 e^{l(l+1)\theta^2_{\rm FWHM}/8\ln 2} , \\ C_l^{EE}\big|_{\rm noise} &= C_l^{BB}\big|_{\rm noise} = \left(\frac{\Delta_\Theta}{T_{\rm CMB}} \right)^2 e^{l(l+1)\theta^2_{\rm FWHM}/8\ln 2} , \end{aligned} \tag{25}$$

where Δ_Θ and Δ_P characterize detector noise, and $\theta_{\rm FWHM}$ is the FWHM of the beam. We employ the specifications of a nearly ideal reference experiment, with $\Delta_\Theta = 1\mu$K-arcmin, $\Delta_P = \sqrt{2}\mu$K-arcmin, and $\theta_{\rm FWHM} = 4'$ (see [10] for an exploration of noise properties).

If we instead consider an ensemble of CMB fields lensed by a *fixed* deflection field, the multipole covariance acquires off-diagonal terms of the form

$$\langle a_l^m b_{l'}^{m'} \rangle \Big|_{\rm lens} = \sum_{LM} (-1)^M \begin{pmatrix} l & l & L \\ m & m' & -M \end{pmatrix} f^\alpha_{lLl'} \phi_L^M , \tag{26}$$

where the subscript indicates that we consider a fixed lensing field. $f^\alpha_{lLl'}$ are weights for the different quadratic pairs denoted by α, given by

$$f^\alpha_{l_1 L l_2} = {}_{s_a}F_{l_1 L l_2} \left[\epsilon_{l_1 l_2 L} \tilde{C}^{ab}_{l_2} + \beta_{l_1 l_2 L} \tilde{C}^{b\bar{a}}_{l_2} \right] + {}_{s_b}F_{l_2 L l_1} \left[\epsilon_{l_1 l_2 L} \tilde{C}^{ab}_{l_1} - \beta_{l_1 l_2 L} \tilde{C}^{a\bar{b}}_{l_1} \right] , \tag{27}$$

where s_a and s_b are the spins of the a and b fields respectively. Specific forms for the six quadratic pairs are given in Table I.

α	$f^\alpha_{l_1 L l_2}$
$\Theta\Theta$	$\tilde{C}^{\Theta\Theta}_{l_1} {}_0F_{l_2 L l_1} + \tilde{C}^{\Theta\Theta}_{l_2} {}_0F_{l_1 L l_2}$
ΘE	$\tilde{C}^{\Theta E}_{l_1} {}_2F_{l_2 L l_1} + \tilde{C}^{\Theta E}_{l_2} {}_0F_{l_1 L l_2}$, even
EE	$\tilde{C}^{EE}_{l_1} {}_2F_{l_2 L l_1} + \tilde{C}^{EE}_{l_2} {}_2F_{l_1 L l_2}$, even
ΘB	$i\tilde{C}^{\Theta E}_{l_1} {}_2F_{l_2 L l_1}$, odd
EB	$i\left[\tilde{C}^{EE}_{l_1} {}_2F_{l_2 L l_1} - \tilde{C}^{BB}_{l_2} {}_2F_{l_1 L l_2}\right]$, odd
BB	$\tilde{C}^{BB}_{l_1} {}_2F_{l_2 L l_1} + \tilde{C}^{BB}_{l_2} {}_2F_{l_1 L l_2}$, even

TABLE I: Functional forms for $f^\alpha_{l_1 L l_2}$. "Even" and "odd" indicate that the functions are non-zero only when $L + l_1 + l_2$ is even or odd, respectively.

Because ϕ_L^M is itself a zero mean field, the two-point correlations $\langle a_l^m b_{l'}^{m'} \rangle$ taken over the ensemble would vanish. In a given realization, we can however construct an estimator for the deflections as a weighted sum over multipole pairs, and find weights that minimize the variance of the estimator. We write a general weighted sum of multipole pairs as

$$d^{\alpha}{}_L^M = \frac{A_L^\alpha}{\sqrt{L(L+1)}} \sum_{l_1 m_1} \sum_{l_2 m_2} (-1)^M \begin{pmatrix} l_1 & l_2 & L \\ m_1 & m_2 & -M \end{pmatrix} g^\alpha_{l_1 l_2}(L) a_{l_1}^{m_1} b_{l_2}^{m_2} , \tag{28}$$

where a_l^m and b_l^m are lensed CMB fields, and α simply denotes the specific choice of a and b. The minimum variance estimator is obtained by finding the weights $g^{\alpha}_{l_1 l_2}(L)$ that minimizes the Gaussian variance $\langle d^{\alpha}{}_L^{M*} d^{\alpha}{}_L^{M}\rangle$ subject to the constraint

$$\langle d^{\alpha}{}_L^{M}\rangle\big|_{\rm lens} = \sqrt{L(L+1)}\phi_L^M. \tag{29}$$

The filter takes the form

$$g^{\alpha}_{l_1 l_2}(L) = \frac{C^{aa}_{l_2} C^{bb}_{l_1} f^{\alpha *}_{l_1 L l_2} - (-1)^{L+l_1+l_2} C^{ab}_{l_1} C^{ab}_{l_2} f^{\alpha *}_{l_2 L l_1}}{C^{aa}_{l_1} C^{aa}_{l_2} C^{bb}_{l_1} C^{bb}_{l_2} - (C^{ab}_{l_1} C^{ab}_{l_2})^2}, \tag{30}$$

with constraint (29) satisfied with normalization

$$A^{\alpha}_L = L(L+1)(2L+1)\left\{\sum_{l_1 l_2} g^{\alpha}_{l_1 l_2}(L) f^{\alpha *}_{l_1 L l_2}\right\}^{-1}. \tag{31}$$

Note that for $a = b$,

$$g^{\alpha}_{l_1 l_2}(L) \to \frac{f^{\alpha *}_{l_1 L l_2}}{2 C^{aa}_{l_1} C^{aa}_{l_2}}, \tag{32}$$

and for $C_l^{ab} = 0$ (e.g., for ΘB or EB),

$$g^{\alpha}_{l_1 l_2}(L) \to \frac{f^{\alpha *}_{l_1 L l_2}}{C^{aa}_{l_1} C^{bb}_{l_2}}. \tag{33}$$

The Gaussian noise covariance

$$\langle d^{\alpha}{}_L^{M*} d^{\beta}{}_{L'}^{M'}\rangle \equiv \delta_{L,L'}\delta_{M,M'}\left[C_L^{dd} + N_L^{\alpha\beta}\right] \tag{34}$$

is given by

$$N_L^{\alpha\beta} = \frac{A_L^{\alpha *} A_L^{\beta}}{L(L+1)(2L+1)} \sum_{l_1 l_2}\left\{ g^{\alpha *}_{l_1 l_2}(L)\left[C^{ac}_{l_1} C^{bd}_{l_2} g^{\beta}_{l_1 l_2}(L) + (-1)^{L+l_1+l_2} C^{ad}_{l_1} C^{bc}_{l_2} g^{\beta}_{l_2 l_1}(L)\right]\right\}, \tag{35}$$

with $\alpha = (ab)$, $\beta = (cd)$. For $\alpha = \beta$, the above reduces simply to $N_L^{\alpha\alpha} = A_L^{\alpha}$.

Following the treatment of the flat sky case in [10], we form a minimum variance estimator out of the measured quadratic pairs according to

$$d^{\rm mv}{}_L^M = \sum_{\alpha} w^{\alpha}(L) d^{\alpha}{}_L^M, \tag{36}$$

with variance

$$N_L^{\rm mv} = \frac{1}{\sum_{\alpha\beta}\left(\mathbf{N}_L^{-1}\right)^{\alpha\beta}}, \tag{37}$$

and weights

$$w^{\alpha}(L) = N_L^{\rm mv}\sum_{\beta}\left(\mathbf{N}_L^{-1}\right)^{\alpha\beta}. \tag{38}$$

We will hereafter ignore contributions from the BB estimator, since the primordial contributions to the B-mode power spectrum is expected to be small on scales where the lensed multipoles are employed.

We plot the noise power spectra for the five estimators, as well as the minimum variance estimator, in Fig. 1, assuming the noise properties of the reference experiment. Fig. 2 shows fractional differences between the noise in flat sky estimators derived in [10] and the noise in full sky estimators, defined as $\delta N_L^{\alpha}/N_L^{\alpha} \equiv (N_L^{\alpha({\rm flat})} - N_L^{\alpha({\rm full})})/N_L^{\alpha({\rm full})}$. Because most of the information comes from multipole pairs at high multipole moments, the flat sky expressions deviate at less than $\sim 1\%$ for $L > 200$, mainly in the direction of overestimating the noise.

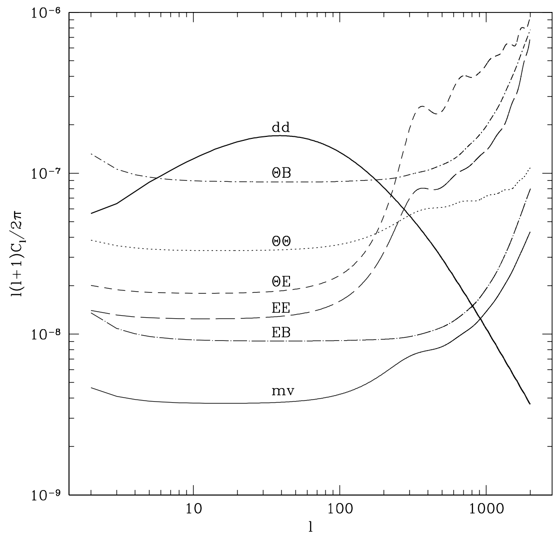

FIG. 1: Deflection and noise power spectra for the quadratic and minimum variance estimators, assuming the noise properties of the reference experiment ($\Delta_\Theta = 1\mu$K-arcmin; $\Delta_P = \sqrt{2}\mu$K-arcmin; $\theta_{\rm FWHM} = 4'$) and a fiducial ΛCDM cosmology with with parameters $\Omega_c = 0.3$, $\Omega_b = 0.05$, $\Omega_\Lambda = 0.65$, $h = 0.65$, $n = 1$, $\delta_H = 4.2 \times 10^{-5}$ and no gravitational waves.

IV. EFFICIENT ESTIMATORS

The quadratic estimators involve both filtering and convolution in harmonic space. It is useful in practice to express the convolution as a product of the fields in angular space. The estimators can then be constructed using fast harmonic transform algorithms [21, 22]. To simplify the construction of the estimators we will assume $\tilde{C}_l^{BB} \ll \tilde{C}_l^{EE}$ as is appropriate for the standard cosmology. Aside from the EB estimator, derived in [10] under the flat sky approximation, the angular space estimators involving polarization are new to this work.

Generalizing the construction in [7] for the $\Theta\Theta$ estimator, consider the fact that lensing correlates the (lensed) temperature and polarization fields to the their (unlensed) angular gradients. We show in Appendix A that the all-sky analog to the gradient operation on a spin-s field is $\partial_i \to D_i$. The quadratic estimator is then built out of the

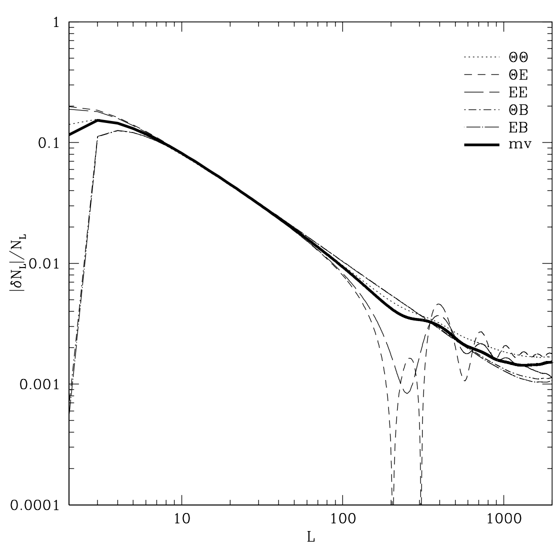

FIG. 2: Fractional differences $\delta N_L/N_L$ between the noise in the flat sky and full sky estimators, calculated for the reference experiment.

general operation on two fields $X(\hat{\boldsymbol{n}})$ and $Y(\hat{\boldsymbol{n}})$

$$P[X(\hat{\boldsymbol{n}}), Y(\hat{\boldsymbol{n}})] \equiv -D^i[X(\hat{\boldsymbol{n}})D_iY(\hat{\boldsymbol{n}})]\,. \tag{39}$$

The properly normalized estimators then take the form

$$\hat{d}^{\alpha M}_{\ L} = \frac{\hat{A}^\alpha_L}{\sqrt{L(L+1)}}\int d\hat{\boldsymbol{n}} Y_L^{M*}(\hat{\boldsymbol{n}}) e^\alpha(\hat{\boldsymbol{n}})\,, \tag{40}$$

where

$$\begin{aligned}
e^{\Theta\Theta}(\hat{\boldsymbol{n}}) &= P[{}_0A_\Theta, {}_0A_{\Theta\Theta}]\,,\\
e^{\Theta E}(\hat{\boldsymbol{n}}) &= \frac{1}{2}\left(P[{}_{+2}A_E, {}_{-2}A_{\Theta E}] + P[\mathrm{cc}]\right) + P[{}_0A_\Theta, {}_0A_{E\Theta}]\,,\\
e^{\Theta B}(\hat{\boldsymbol{n}}) &= \frac{1}{2}\left(P[{}_{+2}A_{iB}, {}_{-2}A_{\Theta E}] + P[\mathrm{cc}]\right)\,,\\
e^{EE}(\hat{\boldsymbol{n}}) &= \frac{1}{2}\left(P[{}_{+2}A_E, {}_{-2}A_{EE}] + P[\mathrm{cc}]\right)\,,\\
e^{EB}(\hat{\boldsymbol{n}}) &= \frac{1}{2}\left(P[{}_{+2}A_{iB}, {}_{-2}A_{EE}] + P[\mathrm{cc}]\right)\,,
\end{aligned} \tag{41}$$

where cc denotes the operation with the complex conjugates of the fields and the filtered fields themselves are given by the general prescription

$$\begin{aligned}
{}_{\pm s}A_X(\hat{\boldsymbol{n}}) &= \sum_{lm}\frac{1}{C_l^{XX}} X_l^m\, {}_{\pm s}Y_l^m(\hat{\boldsymbol{n}}),\\
{}_{\pm s}A_{XY}(\hat{\boldsymbol{n}}) &= \sum_{lm}\frac{\tilde{C}_l^{XY}}{C_l^{XX}} X_l^m\, {}_{\pm s}Y_l^m(\hat{\boldsymbol{n}}).
\end{aligned} \tag{42}$$

We omit the $\alpha = BB$ estimator under the assumption that the unlensed B-power is small at high multipoles.

It is straightforward to verify that all of the estimators are the same as the harmonic space ones $\hat{d}^{\alpha M}_{\ L} = d^{\alpha M}_{\ L}$ with $\hat{A}^\alpha_L = A^\alpha_L$ except for ΘE. Here the weights on the multipole combination are

$$\hat{g}^{\Theta E}_{l_1 l_2} = \frac{f^{\Theta E}_{l_1 L l_2}}{C^{\Theta\Theta}_{l_1} C^{EE}_{l_2}} \tag{43}$$

and are slightly non-optimal. Furthermore $\hat{N}_L \neq \hat{A}_L$ and they must be calculated separately. However a direct calculation of the noise spectrum through Eqn. (35) shows that the differences are less than 1%, and essentially indistinguishable from the optimal estimator (see Fig. 3).

These estimators may therefore be used in place of a direct multipole summation for efficient lens reconstruction. The gradient operations in Eqn. (39) are efficiently evaluated in harmonic space since their action on spin harmonics simply raises and lowers the spin index in accordance with Eqn. (A17).

V. FLAT-SKY APPROXIMATION

The all-sky estimators reduce to the flat sky estimators, based on Fourier harmonics of the fields in the small angle limit. Here we explicitly show this correspondence.

The full sky harmonics in multipole space (l, m) are related to the flat sky harmonics in Fourier space $\boldsymbol{l} = l\cos\phi_l \hat{\boldsymbol{x}} + l\sin\phi_l \hat{\boldsymbol{y}}$ by [13, 23]

$$X(\boldsymbol{l}) = \sqrt{\frac{4\pi}{2l+1}}\sum_m i^{-m} X_l^m e^{im\phi_l}. \tag{44}$$

Rewriting Eq. (28) using the above,

$$\begin{aligned}
d^\alpha(\boldsymbol{L}) \;\approx\; & \frac{A^\alpha_L}{\sqrt{L(L+1)}}\sum_M (-i)^M e^{iM\phi_L}\sum_{l_1 m_1}\sum_{l_2 m_2} i^{m_1+m_2} g^\alpha_{l_1 l_2}(L)\begin{pmatrix} l_1 & l_2 & L\\ m_1 & m_2 & -M\end{pmatrix}\\
&\times\sqrt{\frac{(2l_1+1)(2l_2+1)}{4\pi(2L+1)}}\int\frac{d\phi_1}{2\pi}\frac{d\phi_2}{2\pi} e^{-im_1\phi_1} e^{-im_2\phi_2} a(\boldsymbol{l}_1) b(\boldsymbol{l}_2).
\end{aligned} \tag{45}$$

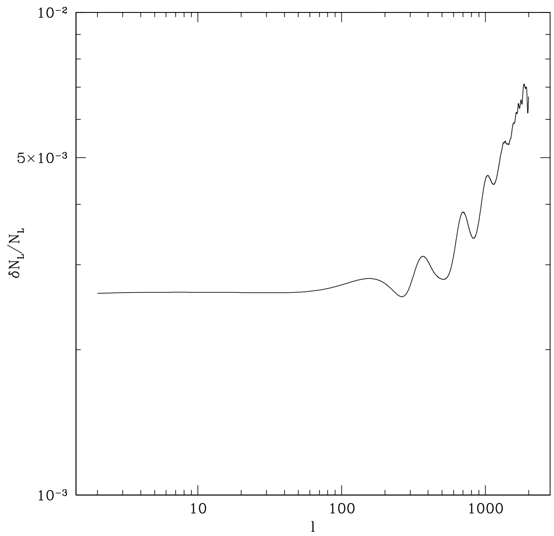

FIG. 3: Fractional difference between the approximate and the optimal ΘE estimators, defined as $\delta N_L/N_L \equiv (N_L^{\rm approx.} - N_L^{\rm optimal})/N_L^{\rm optimal}$.

To go further, we can utilize the approximation [13]

$$\begin{pmatrix} l_1 & L & l_2 \\ 2 & 0 & -2 \end{pmatrix} \approx \begin{pmatrix} l_1 & L & l_2 \\ 0 & 0 & 0 \end{pmatrix} \times \begin{cases} \cos 2(\phi_{l_2} - \phi_{l_1}), & L + l_1 + l_2 = \text{even}, \\ i \sin 2(\phi_{l_2} - \phi_{l_1}), & L + l_1 + l_2 = \text{odd}, \end{cases} \tag{46}$$

with the trigonometric functions defined through the cosine and sine rules, and the $3-j$ symbol on the rhs for the odd case represents a continuation of the analytic expression for the even case

$$\begin{pmatrix} l_a & l_b & l_c \\ 0 & 0 & 0 \end{pmatrix} = (-1)^{l/2} \frac{\left(\frac{l}{2}\right)!}{\left(\frac{l}{2}-l_a\right)!\left(\frac{l}{2}-l_b\right)!\left(\frac{l}{2}-l_c\right)!} \left[\frac{(l-2l_a)!(l-2l_b)!(l-2l_c)!}{(l+1)!}\right]^{1/2}, \tag{47}$$

where $l = l_a + l_b + l_c$.

Furthermore in the limit $l_1, l_2, L \gg 1$,

$$\frac{1}{2}\left[L(L+1) + l_2(l_2+1) - l_1(l_1+1)\right] \approx \boldsymbol{L} \cdot \boldsymbol{l}_2 \tag{48}$$

and so we may absorb the geometric factors in ${}_sF_{l_1 L l_2}$ as

$${}_sF_{l_1 L l_2} \approx \sqrt{\frac{(2L+1)(2l_1+1)(2l_2+1)}{4\pi}} \begin{pmatrix} l_1 & l_2 & L \\ 0 & 0 & 0 \end{pmatrix} {}_s\bar{F}_{l_1 L l_2}. \tag{49}$$

with

$${}_s\bar{F}_{l_1 L l_2} \equiv \boldsymbol{L} \cdot \boldsymbol{l}_2 \times \begin{cases} 1, & s = 0, \\ \cos 2(\phi_{l_2} - \phi_{l_1}), & s = 2, L + l_1 + l_2 = \text{even}, \\ i \sin 2(\phi_{l_2} - \phi_{l_1}), & s = 2, L + l_1 + l_2 = \text{odd}, \end{cases} \tag{50}$$

The approximations for $f^\alpha_{l_1 L l_2}$ and $g^\alpha_{l_1 l_2}(L)$ can likewise be written as

$$\begin{aligned} f^\alpha_{l_1 L l_2} &\approx \sqrt{\frac{(2L+1)(2l_1+1)(2l_2+1)}{4\pi}} \begin{pmatrix} l_1 & l_2 & L \\ 0 & 0 & 0 \end{pmatrix} \bar{f}^\alpha_{l_1 L l_2}, \\ g^\alpha_{l_1 l_2}(L) &\approx \sqrt{\frac{(2L+1)(2l_1+1)(2l_2+1)}{4\pi}} \begin{pmatrix} l_1 & l_2 & L \\ 0 & 0 & 0 \end{pmatrix} \bar{g}^\alpha_{l_1 l_2}(L), \end{aligned} \tag{51}$$

where $\bar{f}^{\alpha}_{l_1 L l_2}$ and $\bar{g}^{\alpha}_{l_1 l_2}(L)$ are defined as the unbarred quantities with ${}_sF_{l_1 L l_2}$ replaced by ${}_s\bar{F}_{l_1 L l_2}$. We also list two relations which will prove useful:

$$\begin{pmatrix} l_1 & l_2 & L \\ 0 & 0 & 0 \end{pmatrix}\begin{pmatrix} l_1 & l_2 & L \\ m_1 & m_2 & -M \end{pmatrix} = \sqrt{\frac{4\pi}{(2L+1)(2l_1+1)(2l_2+1)}}\int d\hat{\boldsymbol{n}} Y^{m_1}_{l_1}(\hat{\boldsymbol{n}})Y^{m_2}_{l_2}(\hat{\boldsymbol{n}})Y^{-M}_{L}(\hat{\boldsymbol{n}}), \tag{52}$$

$$e^{i\boldsymbol{l}\cdot\hat{\boldsymbol{n}}} \approx \sqrt{\frac{2\pi}{l}}\sum_m i^m Y^m_l e^{-im\phi_l}. \tag{53}$$

Using Eq. (51) to rewrite Eq. (45), and applying relations (52) and (53), the estimator becomes

$$d^{\alpha}(\boldsymbol{L}) \approx \frac{A^{\alpha}_L}{\sqrt{L(L+1)(2L+1)}}\sum_{l_1 l_2}\bar{g}^{\alpha}_{l_1 l_2}(L)\sqrt{\frac{(2l_1+1)(2l_2+1)}{4\pi}} \times \int \frac{d\phi_1}{2\pi}\frac{d\phi_2}{2\pi}\sqrt{\frac{l_1 l_2 L}{(2\pi)^3}}a(\boldsymbol{l}_1)b(\boldsymbol{l}_2)\int d\hat{\boldsymbol{n}} e^{i(\boldsymbol{l}_1+\boldsymbol{l}_2+\boldsymbol{L})\cdot\hat{\boldsymbol{n}}}. \tag{54}$$

Taking $l_1, l_2, L \gg 1$, the above reduces to

$$d^{\alpha}(\boldsymbol{L}) \approx \frac{A^{\alpha}_L}{L}\int \frac{d^2\boldsymbol{l}_1}{(2\pi)^2}\bar{g}^{\alpha}_{l_1 l_2}(L)a(\boldsymbol{l}_1)b(\boldsymbol{l}_2), \quad \boldsymbol{l}_2 = \boldsymbol{L} - \boldsymbol{l}_1 \tag{55}$$

with $\bar{g}^{\alpha}_{l_1 l_2}(L)$ corresponding to the filters $F_{\alpha}(\boldsymbol{l}_1, \boldsymbol{l}_2)$ in [10]. The normalization A^{α}_L reduces to the flat sky expression in [10] in a similar fashion, by using the approximations (51) to relate the full sky quantities to trigonometric functions on the flat sky.

It is simple to show that the efficient all-sky estimator in Eqn. (40) reduces to efficient flat sky estimators with the replacements $D_i \to \partial_i$ in Eqn. (39) and the spherical harmonic transform in Eqn. (40) with a Fourier transform. Under the assumption of $\tilde{C}^{BB}_l \ll \tilde{C}^{EE}_l$, they again reproduce the properties of the minimum variance quadratic estimators in Eqn. (55) and allow fast Fourier transform techniques to be employed in their construction.

VI. DISCUSSION

Counterintuitively, the gravitational lensing of the CMB temperature and polarization fields is a small scale manifestation of the very large scale properties of the intervening mass distribution. It therefore requires very challenging, high angular resolution ($< 10'$) but wide-field surveys ($>$ few degrees) to exploit. We have provided expressions for quadratic estimators of the lensing potential valid on the entire sky, as well as the expected noise covariances for the estimators. As expected, on small angular scales ($L \geq 100$), the flat sky approximations differ from the full sky expressions by less than $\sim 1\%$, indicating that the flat sky approximations is adequate. This regime is however not where the signal-to-noise peaks.

We have also provided a practical means of implementing these estimators using fast harmonic transforms, either with spherical harmonics or Fourier harmonics, to perform the required harmonic convolutions and filtering. We have shown that even the approximate ΘE estimator has a noise performance that is essentially indistinguishable from optimal. These techniques should provide a means to study the impact of real world issues such as finite-field, inhomogeneous noise, and foregrounds on the science of CMB lensing.

Acknowledgments

This work was supported by NASA NAG5-10840 and the DOE OJI program.

APPENDIX A: TENSOR REPRESENTATION OF SPIN WEIGHTED FUNCTIONS

We clarify the relation between spin-s functions and tensor quantities on the sphere, and derive the relation between spin raising and lowering operators and covariant derivatives on the sphere.

Suppose we construct an orthonormal basis $(\hat{\boldsymbol{e}}_1(\hat{\boldsymbol{n}}), \hat{\boldsymbol{e}}_2(\hat{\boldsymbol{n}}))$ at each point on the sphere. We define a local rotation as a right-handed rotation of the basis vectors $(\hat{\boldsymbol{e}}_1, \hat{\boldsymbol{e}}_2)$ by an angle ψ, so that the new basis vectors $(\hat{\boldsymbol{e}}_{1'}, \hat{\boldsymbol{e}}_{2'})$ are related to the original vectors by the transformation

$$\begin{aligned} \hat{\boldsymbol{e}}_{1'} &= \cos\psi \hat{\boldsymbol{e}}_1 - \sin\psi \hat{\boldsymbol{e}}_2, \\ \hat{\boldsymbol{e}}_{2'} &= \sin\psi \hat{\boldsymbol{e}}_1 + \cos\psi \hat{\boldsymbol{e}}_2. \end{aligned} \tag{A1}$$

A function ${}_sf(\hat{\boldsymbol{n}})$ is said to carry a spin-weight s if, under the rotation (A1), the function transforms as ${}_sf(\hat{\boldsymbol{n}}) \to e^{-is\phi}{}_sf(\hat{\boldsymbol{n}})$. This convention conforms to [15], and defines rotations in a sense opposite to that in [17, 24].

We define vectors $\boldsymbol{m}$ and $\bar{\boldsymbol{m}}$ with respect to the basis $(\hat{\boldsymbol{e}}_1, \hat{\boldsymbol{e}}_2)$ according to

$$\boldsymbol{m} = \frac{1}{\sqrt{2}}\left[\hat{\boldsymbol{e}}_1 + i\hat{\boldsymbol{e}}_2\right], \tag{A2}$$

$$\bar{\boldsymbol{m}} = \frac{1}{\sqrt{2}}\left[\hat{\boldsymbol{e}}_1 - i\hat{\boldsymbol{e}}_2\right], \tag{A3}$$

which have the property that

$$\begin{aligned} \boldsymbol{m}\cdot\boldsymbol{m} &= \bar{\boldsymbol{m}}\cdot\bar{\boldsymbol{m}} = 0, \\ \boldsymbol{m}\cdot\bar{\boldsymbol{m}} &= 1. \end{aligned} \tag{A4}$$

Given a vector field $\hat{\boldsymbol{v}}(\hat{\boldsymbol{n}})$, it can easily be shown that the quantities $\boldsymbol{v}\cdot\boldsymbol{m}$ and $\boldsymbol{v}\cdot\bar{\boldsymbol{m}}$ transform as spin 1 and -1 objects, respectively, so that $\boldsymbol{m}$ and $\bar{\boldsymbol{m}}$ act as spin projection vectors. More generally, given a rank-s tensor $T_{i_1\ldots i_s}$, the quantity $T_{i_1\ldots i_s}\boldsymbol{m}^{i_1}\cdots\boldsymbol{m}^{i_s}$ transforms as a spin-s object, since under the rotation (A1), each factor of $\boldsymbol{m}^{i_n}$ contributes a phase $e^{-is\psi}$.

The spin-s functions ${}_sf(\hat{\boldsymbol{n}})$ therefore also provide a complete basis for the totally symmetric trace-free portion of a rank-s tensor

$$T_{i_1\ldots i_s} = {}_sf(\hat{\boldsymbol{n}})\bar{\boldsymbol{m}}_{i_1}\cdots\bar{\boldsymbol{m}}_{i_s} + {}_{-s}f(\hat{\boldsymbol{n}})\boldsymbol{m}_{i_1}\cdots\boldsymbol{m}_{i_s}, \tag{A5}$$

where the trace-free condition refers to the vanishing under contraction of any two indices in the tensor. For example, the polarization tensor can be written as

$$\mathcal{P}_{ij} = {}_{+2}A(\hat{\boldsymbol{n}})\bar{\boldsymbol{m}}_i\bar{\boldsymbol{m}}_j + {}_{-2}A(\hat{\boldsymbol{n}})\boldsymbol{m}_i\boldsymbol{m}_j. \tag{A6}$$

Covariant differentiation of such a tensor is related to the raising and lowering of the spin weight [17]:

$$\begin{aligned} \nabla_k T_{i_1\ldots i_s} &= \left[\partial_{k\,s}f(\hat{\boldsymbol{n}})\right]\bar{\boldsymbol{m}}_{i_1}\cdots\bar{\boldsymbol{m}}_{i_s} + {}_sf(\hat{\boldsymbol{n}})\nabla_{(k}\bar{\boldsymbol{m}}_{i_1}\cdots\bar{\boldsymbol{m}}_{i_s)} \\ &+ \left[\partial_{k\,-s}f(\hat{\boldsymbol{n}})\right]\boldsymbol{m}_{i_1}\cdots\boldsymbol{m}_{i_s} + {}_{-s}f(\hat{\boldsymbol{n}})\nabla_{(k}\boldsymbol{m}_{i_1}\cdots\boldsymbol{m}_{i_s)}. \end{aligned} \tag{A7}$$

We evaluate the covariant derivatives $\nabla_i\bar{\boldsymbol{m}}_j$ etc. explicitly in the spherical basis with coordinates (θ, ϕ), yielding

$$\begin{aligned} \nabla_\theta\bar{\boldsymbol{m}}_\theta &= \nabla_\theta\bar{\boldsymbol{m}}_\varphi = 0, \\ \nabla_\varphi\bar{\boldsymbol{m}}_\theta &= \frac{i}{\sqrt{2}}\cos\theta, \\ \nabla_\varphi\bar{\boldsymbol{m}}_\varphi &= \frac{1}{\sqrt{2}}\sin\theta\cos\theta, \end{aligned} \tag{A8}$$

with those for $\boldsymbol{m}$ given as complex conjugates of the above. Using these, it can be shown that

$$\begin{aligned} \bar{\boldsymbol{m}}^j\nabla_i\bar{\boldsymbol{m}}_j &= \boldsymbol{m}^j\nabla_i\boldsymbol{m}_j = 0, \\ \boldsymbol{m}^j\nabla_i\bar{\boldsymbol{m}}_j &= -\bar{\boldsymbol{m}}^j\nabla_i\boldsymbol{m}_j = J_i, \end{aligned} \tag{A9}$$

where

$$J_\theta = 0, \qquad J_\phi = i\cos\theta, \tag{A10}$$

in spherical coordinates. The covariant derivative of $T_{i_1\ldots i_s}$ is therefore given by

$$\nabla_k T_{i_1\ldots i_s} = \left[D_k\,{}_sf(\hat{\boldsymbol{n}})\right]\bar{\boldsymbol{m}}_{i_1}\cdots\bar{\boldsymbol{m}}_{i_s} + \left[D_k\,{}_{-s}f(\hat{\boldsymbol{n}})\right]\boldsymbol{m}_{i_1}\cdots\boldsymbol{m}_{i_s}, \tag{A11}$$

where we define the spin-dependent gradient operator as

$$D_i \equiv \partial_i + sJ_i. \tag{A12}$$

A covariant derivative ∇_i operating on the spin-s piece of a tensor is equivalent to a gradient operation D_i on its spin-s weighted representation. As an example, the components of the covariant derivative of the polarization tensor

$$\begin{aligned} \boldsymbol{m}^i \boldsymbol{m}^j \nabla_k \mathcal{P}_{ij} &= D_k[{}_2A(\hat{\boldsymbol{n}})], \\ \bar{\boldsymbol{m}}^i \bar{\boldsymbol{m}}^j \nabla_k \mathcal{P}_{ij} &= D_k[{}_{-2}A(\hat{\boldsymbol{n}})]. \end{aligned} \tag{A13}$$

The gradient operator D_k is related to spin raising and lowering operators. Using the expressions (A10) and expressing the operator D_k in the $(\boldsymbol{m}, \bar{\boldsymbol{m}})$ basis, we obtain the desired relations

$$D_i\left[{}_sf(\hat{\boldsymbol{n}})\right] = -\frac{1}{\sqrt{2}}\left\{\left[\eth_s f(\hat{\boldsymbol{n}})\right]\bar{\boldsymbol{m}}_i + \left[\bar{\eth}_s f(\hat{\boldsymbol{n}})\right]\boldsymbol{m}_i\right\}. \tag{A14}$$

By virtue of the rotational properties of $(\boldsymbol{m}, \bar{\boldsymbol{m}})$, the ladder operators $\eth$ and $\bar{\eth}$, defined by [17, 24]

$$\eth_s f(\theta,\varphi) = -\sin^s\theta\left[\frac{\partial}{\partial\theta} + i\csc\theta\frac{\partial}{\partial\varphi}\right]\sin^{-s}\theta_s f(\theta,\varphi), \tag{A15}$$

$$\bar{\eth}_s f(\theta,\varphi) = -\sin^{-s}\theta\left[\frac{\partial}{\partial\theta} - i\csc\theta\frac{\partial}{\partial\varphi}\right]\sin^{s}\theta_s f(\theta,\varphi), \tag{A16}$$

raise and lower the spin weight by 1. For example, the gradient operation on the spin-s spherical harmonic yields

$$D_i[{}_sY_l^m] = -\frac{1}{\sqrt{2}}\left([(l-s)(l+s+1)]^{1/2}{}_{s+1}Y_l^m\bar{\boldsymbol{m}}_i - [(l+s)(l-s+1)]^{1/2}{}_{s-1}Y_l^m\boldsymbol{m}_i\right). \tag{A17}$$

Note that the inner product of two gradients

$$[D^i{}_{s_1}f_1(\hat{\boldsymbol{n}})][D_i{}_{s_2}f_2(\hat{\boldsymbol{n}})] = \frac{1}{2}\left\{[\bar{\eth}_{s_1}f_1(\hat{\boldsymbol{n}})][\eth_{s_2}f_2(\hat{\boldsymbol{n}})] + [\eth_{s_1}f_1(\hat{\boldsymbol{n}})][\bar{\eth}_{s_2}f_2(\hat{\boldsymbol{n}})]\right\} \tag{A18}$$

leaves the total spin-weight of the product unchanged.

Inverting the relation (A14), we obtain the ladder operators in the tensor representation

$$\eth_s f(\hat{\boldsymbol{n}}) = -\sqrt{2}\boldsymbol{m}^j\boldsymbol{m}^{i_1}\cdots\boldsymbol{m}^{i_s}\nabla_j T_{i_1\ldots i_s}, \tag{A19}$$

$$\bar{\eth}_s f(\hat{\boldsymbol{n}}) = -\sqrt{2}\bar{\boldsymbol{m}}^j\boldsymbol{m}^{i_1}\cdots\boldsymbol{m}^{i_s}\nabla_j T_{i_1\ldots i_s}, \tag{A20}$$

for $s \geq 0$, and with $\boldsymbol{m}^{i_n}$ replaced by $\bar{\boldsymbol{m}}^{i_n}$ for $s < 0$. This relationship was first proven in [17], albeit with a different sign convention.

---

[1] U. Seljak, Astrophys. J. **463**, 1 (1996).
[2] M. Zaldarriaga and U. Seljak, Phys. Rev. D **58**, 023003 (1998).
[3] F. Bernardeau, Astron. & Astrophys. **324**, 15 (1997).
[4] F. Bernardeau, Astron. & Astrophys. **338**, 375 (1998).
[5] M. Zaldarriaga and U. Seljak, Phys. Rev. D **59**, 123507 (1999).
[6] J. Guzik, U. Seljak, and M. Zaldarriaga, Phys. Rev. D **62**, 043517 (2000).
[7] W. Hu, Phys. Rev. D **64**, 083005 (2001).
[8] W. Hu, Astrophys. J. Lett **557**, L79 (2001).
[9] C.M. Hirata and U. Seljak, Phys. Rev. D in press, astro-ph/0209489 (2002).
[10] W. Hu and T. Okamoto, Astrophys. J. **574**, 566 (2002).
[11] L. Knox and Y. S. Song, Phys. Rev. Lett. **89**, 011303 (2002).
[12] M. Kesden, A. Cooray, and M. Kamionkowski, Phys. Rev. Lett. **89**, 011304 (2002).
[13] W. Hu, Phys. Rev. D **62**, 043007 (2000).
[14] A. Challinor and G. Chon, Phys. Rev. D in press, (2000).
[15] M. Zaldarriaga and U. Seljak, Phys. Rev. D **55**, 1830 (1997).
[16] M. Kamionkowski, A. Kosowsky, and A. Stebbins, Phys. Rev. D **55**, 7368 (1997).

[17] J. N. Goldberg *et al.*, J. Math. Phys. **8**, 2155 (1967).
[18] A. Blanchard and J. Schneider, Astron. & Astrophys. **184**, 1 (1987).
[19] D.M. Goldberg and D.N. Spergel, Phys. Rev. D **59**, 103002 (1999).
[20] L. Knox, Phys. Rev. D **52**, 4307 (1995).
[21] K.M. Gorski et al., preprint astro-ph/9905275, (1999).
[22] P.F. Muciaccia, P. Natoli, and N. Vittorio, Astrophys. J. **488**, 63 (1997).
[23] M. White, J.E. Carlstrom, M. Dragovan, and W.L. Holzapfel, Astrophys. J. **514**, 12 (1999).
[24] E. Newman and R. Penrose, J. Math. Phys. **7**, 863 (1966).